JOURNAL OF GEOPHYSICAL RESEARCH, VOL. 101, NO. C4, PAGES 8807-8821, APRIL 15, 1996

Formation and evolution of the surface mixed layer and halocline of the Arctic Ocean

B. Rudels

Institut für Meereskunde, Universität Hamburg, Hamburg, Germany

L. G. Anderson

Department of Analytical and Marine Chemistry, Göteborg University, Göteborg, Sweden

E. P. Jones

Department of Fisheries and Oceans, Bedford Institute of Oceanography, Dartmouth, Nova Scotia, Canada

Abstract. Fresh water from summer ice melt and the total freshwater content of the Arctic Ocean water column above the thermocline are estimated from vertical profiles of temperature and salinity observed on the *I/B Oden* 1991 cruise. The seasonal ice melt ranges from 0.5 m to slightly above 1 m and is moderately uniform over the observation area. Regions of lower melting are seen over the Morris Jesup Plateau. The freshwater content is calculated relative to the salinity just above the thermocline north of the Barents Sea. The freshwater content increases toward the interior of the Arctic Ocean, showing that fresh water is advected from other regions into the observation area. Regions of different freshwater content are separated by fronts over the Nansen-Gakkel Ridge, over the Lomonosov Ridge, and in the western Eurasian Basin between waters derived from the Eurasian and Canadian Basins. Denser water, homogenized north of the Barents Sea, is recognized by a temperature minimum layer. The absence of the temperature minimum near the Nansen-Gakkel Ridge indicates that heat is transferred from the Atlantic Layer over a longer time than the shortest route would allow. This observation can be explained if the layer circulates together with the Atlantic Layer, i.e., toward the east and returns above the Nansen-Gakkel Ridge and along the Amundsen Basin. North of the Laptev Sea, this water formed north of the Barents Sea becomes covered by low-salinity shelf water. The increased freshwater content limits the winter convection, so it no longer reaches the thermocline and an intermediate halocline is formed. The halocline in the Eurasian Basin consists of water originating from winter convection in the Arctic Ocean north of the Barents Sea, which then circulates around the basin. Such a formation mechanism also explains the observed distribution of low NO water. The strong density increase limits vertical exchange, and the vertical diffusion coefficient in the halocline is small ($\sim 1 \times 10^{-6}$ m^2 s^{-1}). The increased temperature of the halocline shows that the heat lost upward by the Atlantic Layer, mainly by double-diffusive convection, is trapped below the mixed layer.

1. Introduction

The upper waters of the Arctic Ocean are characterized by a shallow mixed layer at or near the freezing point overlying a pronounced cold halocline that separates the surface water from the warmer Atlantic Layer. The sources of fresh water in the surface mixed layer and halocline in addition to sea ice meltwater are primarily (1) rivers that add water at the rims of the basins and (2) low-salinity Pacific water that enters through Bering Strait. This addition of fresh water results in a highly stable upper part of the Arctic Ocean water column, limiting the depth of the winter convection and allowing the surface layer to cool to the freezing point. Subsequent cooling leads to ice formation, with a perennial ice cover being established in the central Arctic Ocean.

Paper number 96JC00143.
0148-0227/96/96JC-00143$05.00

The formation of the Arctic Ocean halocline has been the subject of several discussions [e.g., *Coachman and Barnes*, 1962; *Treshnikov and Baranov*, 1976; *Aagaard et al.*, 1981; *Melling and Lewis*, 1982; *Steele et al.*, 1995]. A widely accepted view emphasizes the role of the large continental shelves in maintaining the halocline [*Aagaard et al.*, 1981; *Melling and Lewis*, 1982]. This view holds that the formation of sea ice over the continental shelves produces cold, brine-enriched waters that flow off the shelves into the central regions of the Arctic Ocean, resulting in a cold halocline. Waters entering the halocline from the shelf areas can be traced by their chemical properties that reflect both Atlantic and Pacific sources [e.g., *Jones and Anderson*, 1986]. Ignored in these discussions is how sea ice formation and melting in more central regions influences not only the evolution of the surface mixed layer, but also that of the halocline. In the surface layer, fresh water is removed and stored temporarily as sea ice in winter, then partly reinjected as seasonal ice melt in summer. In winter the insulating effects of the ice cover limit the heat loss to the atmosphere, and in summer the high albedo reduces the amount of ice melt.

In this work the freshwater content in the water column of the Eurasian Basin and its seasonal variability will be determined by examining salinity and temperature profiles and Θ-S curves obtained during the *I/B Oden* 1991 expedition [*Anderson et al.*, 1994]. Additional data from the *I/B Ymer* 1980, and the ARKTIS II/3, ARKTIS IV/3, and ARKTIS IX/4 *FS Polarstern* expeditions will be included (Figure 1). This leads to a discussion of the seasonal sea ice melt, the freshwater storage, and the redistribution of the fresh water by winter convection with its effect on forming, maintaining, and modifying the underlying halocline. Finally, we discuss the relation between basin and shelf processes, the heat balance of the mixed layer and the halocline, and the effects of the upper layer circulation on the NO distribution. (NO is a conservative parameter, defined by *Broecker* [1974] as $9[NO_3] + [O_2]$.)

2. Approach

The upper layer of the central Arctic Ocean above the halocline shows seasonal variations in its characteristics. In summer there is a homogenous, low-salinity summer melt layer with near-freezing temperatures. This layer is the result of seasonal ice melt. It penetrates downward because of wind mixing and ice keel stirring. In fall and winter it is removed by ice formation and brine rejection, and in winter the mixed layer will be isothermal, at the freezing point, and isohaline down to the base of the convection, for example, as seen from the Arctic Internal Wave Experiment (AIWEX) ice camp in late winter in the Canada Basin (Figure 2) [*Anderson and Swift*, 1990]. In the following summer the depth of the previous winter's mixed layer would be indicated by a temperature minimum located below the summer melt layer. Thus we can estimate the depth of the winter mixed layer of the Arctic Ocean from summer temperature and salinity profiles (Figure 3). Identifying the appropriate temperature minimum may involve a degree of arbitrariness, however. On some stations the choice is obvious, on others less so. When difficult stations are found, we examine not just the temperature, but also the salinity profiles. Winter convection leads to homogenization and to a constant with depth salinity profile. A weaker salinity gradient at the same level as a temperature minimum is then an additional sign of the maximum depth of the winter convection. Of the *I/B Oden* 1991 profiles used in this work about 30% would allow for more than one choice of winter mixed layer depth. The ambiguous stations may show no temperature minimum at all (Figure 3c), or they may show several minima (Figure 3d), the latter suggesting advection from neighboring areas with slightly different convection depths and salinities.

We separate the freshwater content of the Arctic Ocean surface layers into the following three "pools": (1) the seasonal ice melt that causes the salinity of the surface layer to decrease below that of the local winter mixed layer, (2) the fresh water contained in

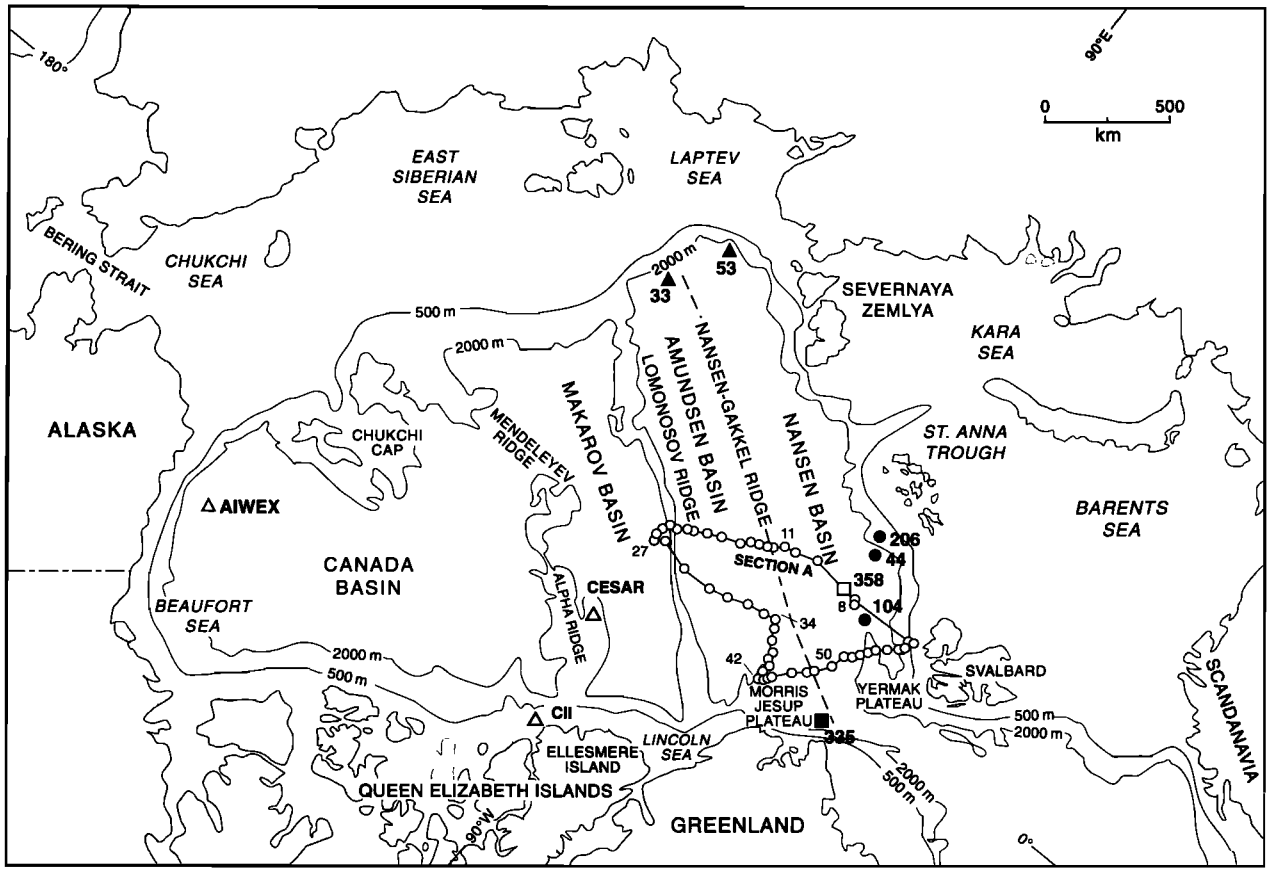

Figure 1. Bathymetric map of the Arctic Ocean. In the Eurasian Basin, stations 104, 44, and 206 (solid circles) are from *Ymer* 80, station 335 (solid square) is from ARKTIS II/3, station 358 (open square) is from ARKTIS IV/3, and stations 33 and 53 (solid triangles) are from ARKTIS IX/3. In the Canada Basin the positions of the ice camps Arctic Internal Wave Experiment (AIWEX), Canadian Expedition to Study the Alpha Ridge (CESAR), and Canadian Ice Island (CII) are noted by open triangles.

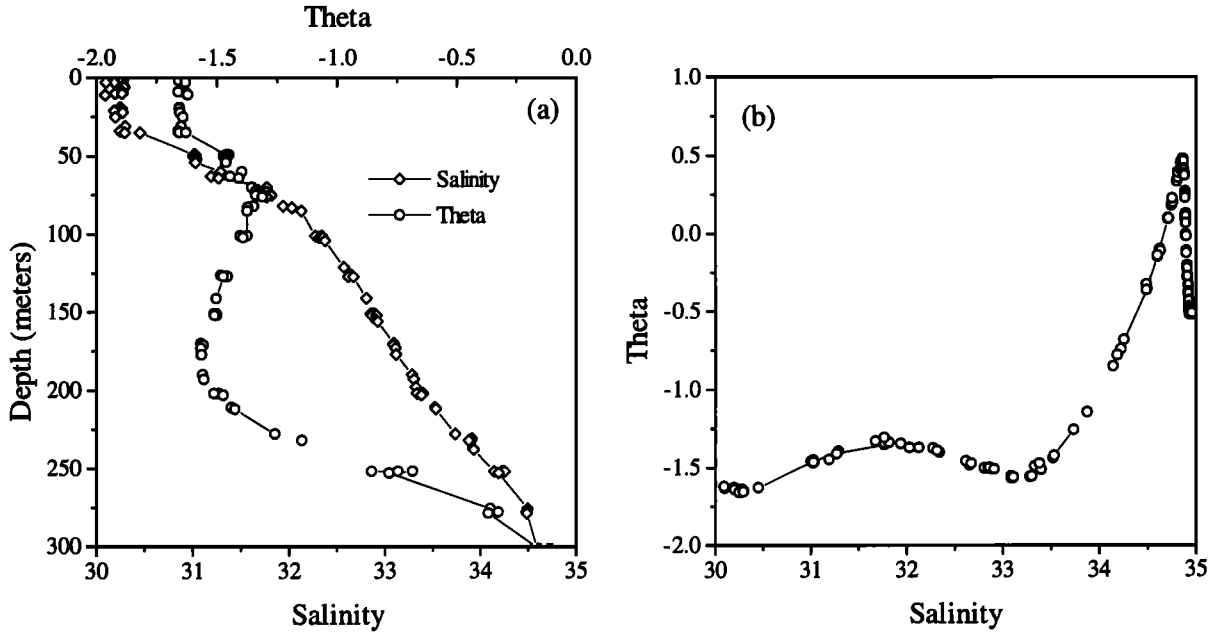

Figure 2. (a) Salinity and potential temperature profiles of the upper 300 m in the Canada Basin and (b) the corresponding Θ-S diagram. The station is taken in late winter from the AIWEX ice camp.

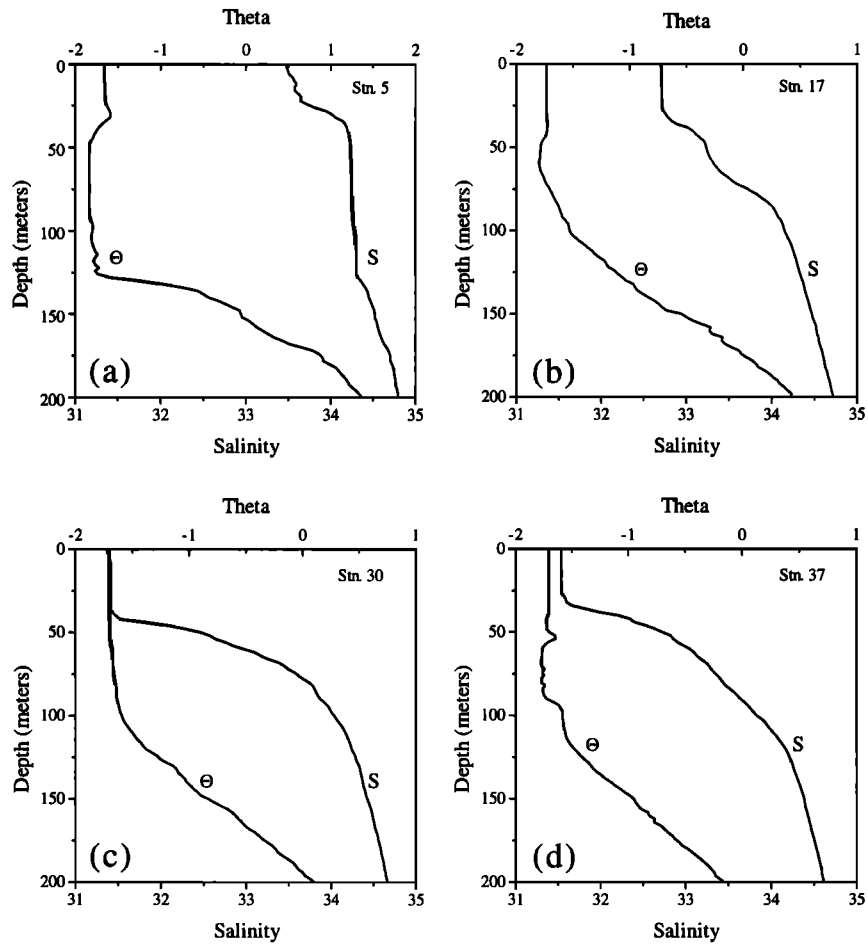

Figure 3. Salinity and temperature profiles for the following *Oden* 91 stations: (a) station 5 in the Nansen Basin north of Svalbard, (b) station 17 in the Amundsen Basin, (c) station 30 in the Amundsen Basin, and (d) station 41 at the tip of the Morris Jesup Plateau. The arrows indicate the chosen depth of the winter mixed layer. The difficulty at some stations to find an unambiguous convection depth as shown in Figures 3c and 3d is obvious.

the winter mixed layer relative to the salinity (S) ≈ 34.3, and (3) the freshwater content between the base of the winter mixed layer and the base of the halocline, here approximated by the S = 34.3 isohaline (Figure 4). The third freshwater pool then gives the freshwater content in the winter halocline below the winter mixed layer. The reason for adopting the value S = 34.3 as the base of the halocline is that it appears to be about the maximum salinity that is attained by the winter mixed layer north of Svalbard, where a homogenization down to the thermocline occurs. This is seen from the Θ-S curves from two stations, one taken by *I/B Ymer* in 1980, the other by *FS Polarstern* in 1987 (Figure 5). As was argued in the introduction and will be substantiated below, this value also indicates the boundary between the thermocline and the Arctic Ocean halocline.

The equivalent depth of fresh water corresponding to the summer ice melt, δH_m, is estimated from

$$\delta H_m = \frac{\left(H_m S_m - \int S(z)dz\right)}{S_m} \quad (1)$$

where H_m and S_m are the depth and salinity of the winter mixed layer, respectively. When performing the calculation, the integral is replaced by a summation over 2 dbar values. The freshwater content in the winter mixed layer δH_W and in the halocline δH_H are determined in a similar manner. Shear is ignored between the winter homogenization and the time of the observation. We can then, at each station, regard the thermodynamic processes as one-dimensional and local as far as the winter-to-summer changes are concerned.

A similar study has been made by *McPhee* [1986] using observations from the Arctic Ice Dynamics Joint Experiment (AIDJEX). He noted that the salinity at 40 m remained constant throughout the summer, then estimated the seasonal ice melt from the salinity reduction above this level. The observations were made from drifting ice camps and included both temporal and spatial variations of the upper water column along the drift track.

The deep homogenous mixed layer north of Svalbard still retains a large fraction of sea ice meltwater relative to the underlying Atlantic Layer. Oxygen 18 measurements point to the mixed layer in this region being primarily produced by ice melt [*Östlund and Hut*, 1984; *Bauch et al.*, 1995]. To compare our results for the freshwater content relative to the Atlantic Water given in most tracer studies, one must add 0.02 times the depth of the 34.3 isohaline. Having formulated the basic features of the approach, we now turn to the description of the freshwater distribution in the different pools as observed on the *I/B Oden* 1991 cruise (Table 1).

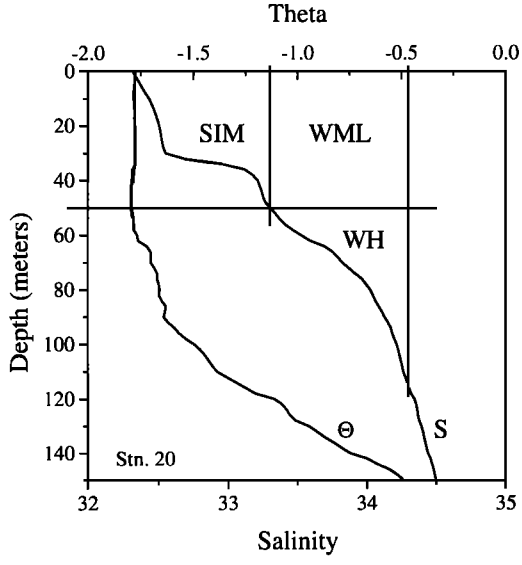

Figure 4. The definition of the three freshwater "pools": seasonal ice melt (SIM), winter surface mixed layer (WSML), and winter halocline (WH).

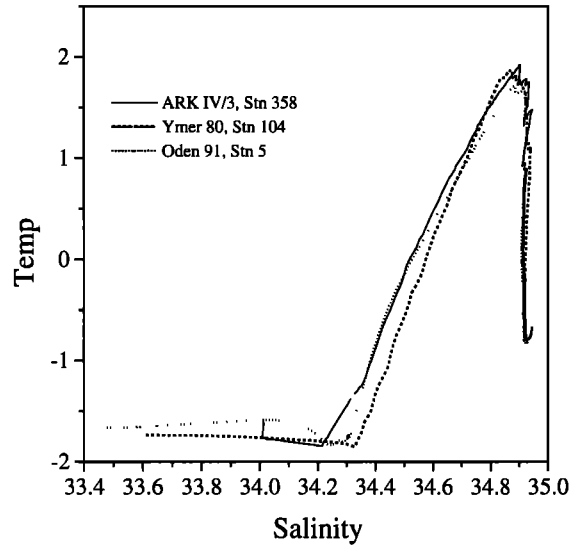

Figure 5. A Θ-S diagram showing stations north of Svalbard taken in 1980 (*Ymer* 80 station 104), 1987 (ARKTIS IV/3, station 358), and 1991 (*Oden* 91 station 5).

3. Seasonal Ice Melt and the Winter Mixed Layer

The spatial variability of the seasonal ice melt and of the freshwater content in the mixed layer and halocline can be appreciated by examining section A running from station 5 in the Nansen Basin to station 27 in the Makarov Basin (Figures 1 and 6). The amount of seasonal ice melt shows some scatter, which can be taken as a measure of the accuracy of the approach. The scatter results mainly from the difficulty in choosing the appropriate temperature minimum in the profiles. While a problem, the error appears to be, at maximum, about 20%. In spite of the station-to-station scatter, a clear pattern emerges. The greatest melting occurs above the ridges (> 1 m) and the least over the basins (< 0.5 m). The lowest ice melt on the section is found in the northern Nansen Basin close to the Nansen-Gakkel Ridge.

The freshwater content in the winter mixed layer is very low in the Nansen Basin. It increases over the Nansen-Gakkel Ridge to the central Amundsen Basin, then remains fairly constant from there to the Lomonosov Ridge. It then rises to the high values (> 2 m) of the Makarov Basin. These successive increases reflect the addition of river runoff to the surface waters and also of low-salinity Pacific Water flowing into the Canadian Basin. The increase in fresh water content along the section is mirrored by a strong decrease in salinity. The addition of freshwater raises the buoyancy of the mixed layer and prevents the winter homogenization from reaching depths as great in the other basins as it does in the Nansen Basin (Figure 6b). The shallower

Table 1. Summary of the Data Evaluated From the Depth Profiles for the Individual Stations

Station	WML				WH	Fresh water content, m			Sensible Heat,	Latent Heat,
	Depth, m	Salinity,	Mean Temperature, °C	Freezing Temperature, °C	Depth, m	SIM	WML	WH	10^6 J m^{-2}	10^6 J m^{-2}
5	124	34.309	-1.757	-1.890	120	0.75	-0.03	0.00	69	252
8	106	34.297	-1.747	-1.890	108	0.83	0.01	0.00	63	278
9	76	34.152	-1.795	-1.881	108	0.28	0.33	0.04	28	95
10	94	34.156	-1.794	-1.881	118	0.48	0.40	0.03	34	160
11	56	33.821	-1.738	-1.862	104	0.49	0.79	0.12	29	164
12	62	33.754	-1.754	-1.858	106	1.17	0.99	0.25	27	393
13	56	33.703	-1.741	-1.856	106	1.05	0.97	0.34	27	352
14	50	33.467	-1.739	-1.842	102	0.75	1.21	0.48	22	250
15	54	33.592	-1.750	-1.849	104	0.80	1.12	0.36	23	267
16	64	33.457	-1.744	-1.841	118	0.90	1.57	0.43	26	301
17	60	33.328	-1.748	-1.834	120	0.76	1.70	0.58	22	256
18	72	33.518	-1.767	-1.845	128	0.94	1.64	0.45	24	317
19	58	33.387	-1.759	-1.838	130	0.75	1.59	0.70	19	251
20	50	33.304	-1.783	-1.833	116	0.91	1.45	0.64	10	305
21	46	33.086	-1.745	-1.820	110	0.69	1.63	0.69	15	233
22	48	33.021	-1.727	-1.817	108	0.96	1.79	0.88	18	321
23	42	32.731	-1.712	-1.800	108	0.82	1.92	0.84	16	276
24	36	32.899	-1.706	-1.810	110	1.16	1.53	1.27	16	389
25	46	32.774	-1.700	-1.803	108	1.34	2.14	0.77	20	448
26	48	32.677	-1.719	-1.797	118	1.15	2.27	1.43	16	386
27	42	32.250	-1.705	-1.773	122	0.75	2.51	1.76	12	252
28	36	32.485	-1.709	-1.786	106	0.84	1.91	1.17	12	281
29	44	32.375	-1.713	-1.780	130	0.98	2.47	1.82	12	328
30	48	32.295	-1.703	-1.795	128	1.24	2.81	1.36	18	415
31	46	32.285	-1.721	-1.775	130	0.68	2.70	1.75	10	227
32	40	32.810	-1.756	-1.805	138	0.66	1.74	1.83	8	222
33	38	32.980	-1.753	-1.814	126	0.89	1.46	1.55	10	300
34	34	32.801	-1.725	-1.804	122	0.79	1.49	1.46	11	265
35	40	32.129	-1.721	-1.766	124	0.53	2.53	1.86	7	176
36	34	32.335	-1.705	-1.778	144	0.66	1.95	2.78	10	221
37	44	32.404	-1.707	-1.782	136	1.02	2.43	1.84	14	340
38	52	32.479	-1.726	-1.786	130	0.84	2.76	1.39	13	283
39	58	32.571	-1.720	-1.791	128	1.24	2.92	1.11	17	414
40	30	31.635	-1.718	-1.738	118	0.21	2.33	2.52	3	69
41	42	31.868	-1.721	-1.751	128	0.25	2.98	1.83	5	83
43	36	31.848	-1.725	-1.750	116	0.19	2.57	1.86	4	64
44	46	32.498	-1.728	-1.787	114	1.02	2.42	0.45	11	341
45	50	32.442	-1.745	-1.784	134	0.83	2.71	1.44	8	278
46	44	33.372	-1.761	-1.837	114	0.50	1.19	0.84	14	167
47	50	33.655	-1.765	-1.853	116	0.46	0.94	0.46	18	155
48	68	33.913	-1.790	-1.868	112	0.56	0.77	0.21	22	187
49	68	33.993	-1.797	-1.872	122	0.63	0.61	0.22	21	211
50	52	33.920	-1.814	-1.868	116	0.84	0.58	0.29	12	280
51	70	33.936	-1.817	-1.869	128	0.75	0.74	0.32	15	251

WML is winter mixed layer, WH is winter halocline, and SIM is seasonal ice melt. Freezing temperature was calculated at the salinity of the WML. The sensible and latent heat in the WML were calculated from the temperature and freshwater content data.

convection allows a winter halocline to build up between the winter mixed layer and the thermocline. The freshwater content in the winter halocline is practically nonexistent in the Nansen Basin, but it increases over the Nansen-Gakkel Ridge. It stays fairly constant in the Amundsen Basin, increasing to more than 1 m in the Makarov Basin on the other side of the Lomonosov Ridge. The increase in freshwater content is accompanied by an increase in the thickness of the winter halocline (difference of the 34.3 and depth of the winter mixed layer lines in Figure 6b).

To obtain a more comprehensive horizontal picture we examine the variation of the different freshwater pools on all the stations occupied during *I/B Oden* in 1991 (Figure 7). The seasonal ice melt is fairly uniform over the region covered. The only exception appears to be the area close to the Morris Jesup Plateau, where less than 0.3 m of ice has melted (see stations 40, 41, and 43 in Table 1). This could be a result of the thick and dense ice field north of Greenland, whose presence would permit little short wave radiation to enter into the leads and whose high albedo would reflect a large part of the radiation hitting the ice. A similar small ice melt was also found on stations occupied by *FS Polarstern* in 1984 close to the Greenland slope (e.g., station 335, Figure 1).

In the area close to Svalbard the low-salinity surface layer is newly formed and has not yet experienced any winter convection. Hence the seasonal ice melt cannot be separated from the melting caused by heat supplied from below by the entering, warm Atlantic Water.

The freshwater content of the winter mixed layer is highest over the Morris Jesup Plateau (> 2.5 m) in spite of the shallow depth of the mixed layer (40 m; see Figures 7b and 7d). In fact,

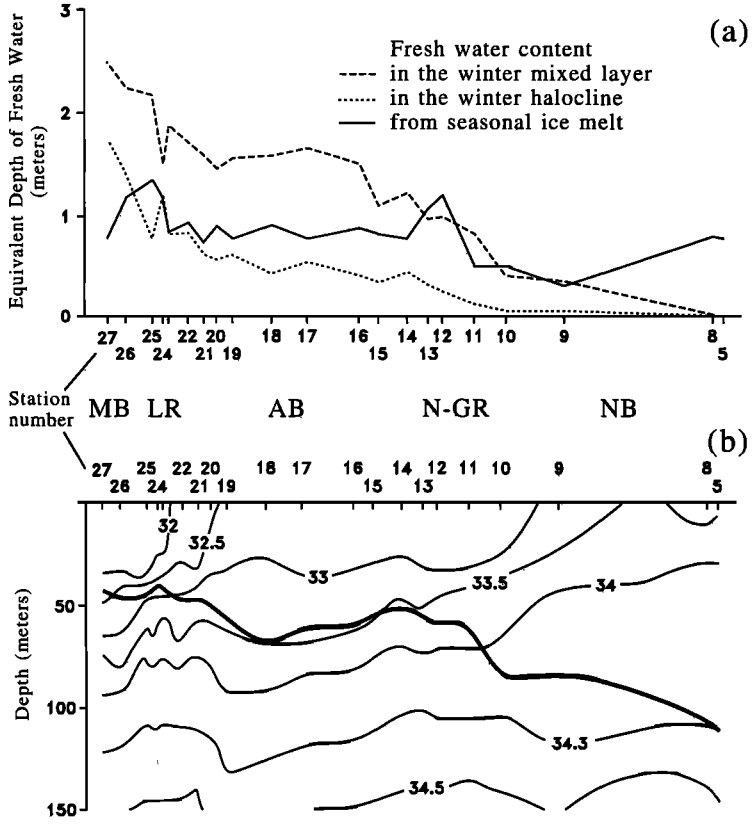

Figure 6. (a) The freshwater content in the three pools and (b) the salinity distribution in the upper 150 along *Oden* 91 section A (Figure 1) from the Nansen Basin into the Makarov Basin. The thick line in Figure 6b indicates the depth of the winter mixed layer. The indication of some geographical references are the Makarov Basin (MB), Lomonosov Ridge (LR), Amundsen Basin (AB), Nansen-Gakkel Ridge (N-GR), and the Nansen Basin (NB)

the entire western part of the Eurasian Basin shows substantially higher amounts of fresh water in the mixed layer. This implies that a large transport of surface water from the Canadian Basin takes place west of section A (Figure 6) and is in agreement with the picture of the surface water following the Transpolar Drift across the Lomonosov Ridge close to the North pole. The low-salinity water appears to accumulate close to the Greenland slope and shelf. The depth and salinity of the mixed layer also indicate the more shallow convection associated with the waters from the Canadian Basin. The freshwater content of the mixed layer close to Fram Strait but away from Greenland again resembles that over the Nansen-Gakkel Ridge and the Amundsen Basin.

The amount of seasonal sea ice melt also gives the amount of heat that has been added to the water column up to the time of the observation. The average value found in the entire observation area, close to 1 m of ice or 335×10^6 J m^{-2} (Figure 7a and Table 1) is of the same order as that found from observations made from ice camps on individual floes [*McPhee*, 1986]. A comparison with measured net incoming radiation during summer, 620×10^6 J m^{-2} [*Vowinckel and Orvig*, 1970], indicates that about 50% of the incoming heat is not included in our estimate. The additional heat is likely going to both heating sea ice and melting sea ice, with the meltwater being stored in melt ponds on top of the ice and in a shallow boundary layer just beneath the ice. Heating the ice would account for 25% of the "missing" heat if we assume that the temperature of a 3-m-thick ice layer is heated by 10°C [*Defant*, 1961]. The remaining missing heat can be accounted for by the production of 0.7 m of melt water that would reside on top of the ice cover or just beneath it. The amount of sensible heat added and stored in the mixed layer is about 20×10^6 J m^{-2} (Table 1), corresponding to an oceanic heat flux of 0.6 W m^{-2} throughout the year. This is about 30% of the 2 W m^{-2} proposed by *Maykut and Untersteiner* [1971] for the oceanic heat loss to the ice.

4. The Winter Halocline

The Θ-S curves from different stations on section A show that the temperature minimum just above the thermocline is observed only in the southern Nansen Basin (Figure 8). In the highest-salinity range (S≈34.3), temperatures are higher and the Θ-S curves are smoother over the Nansen-Gakkel Ridge (station 12) and in the Amundsen Basin (station 17). These observations and the increased freshwater content of the winter mixed layer (Figure 6) allow us to propose a mechanism for the formation of the winter halocline that does not require processes occurring on the shelves [*Aagaard et al.*, 1981] or at the shelf break [*Coachman and Barnes*, 1962]. The proposed mechanism, of course, does not exclude additional contributions from the shelves.

As the Atlantic Water enters the Arctic Ocean through Fram Strait, it encounters and melts sea ice, mainly in the "Whalers Bay" north of Svalbard [*Untersteiner*, 1988]. In winter, cooling and refreezing remove the heat and homogenize the upper layer. Evidence that convective homogenization occurs was found on station 58 during the *I/B Oden* 1991 cruise. With an air temperature of -20°C and strong ice formation occurring during the conductivity-temperature-depth (CTD) cast, a salinity anomaly of 0.3 was observed at 40 m (Figure 9). This parcel of dense water would be capable of sinking to a depth

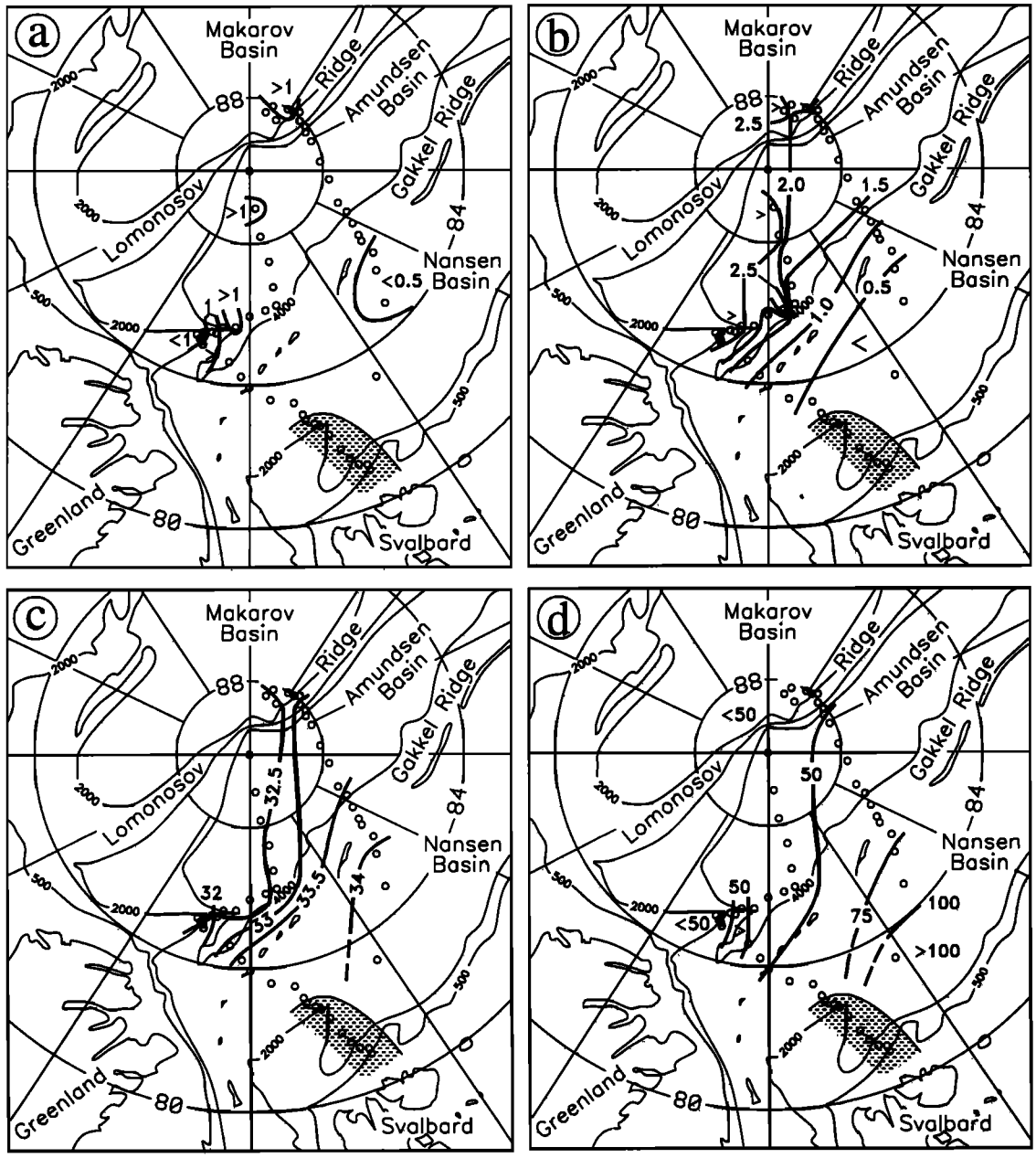

Figure 7. (a) The horizontal distribution of seasonal ice melt, (b) freshwater content in the winter mixed layer, (c) the salinity, and (d) depth of the winter mixed layer in the western Eurasian Basin. The hatched areas indicate the presence of water which has not yet experienced a winter convection and where no winter mixed layer can be identified.

corresponding to that of the top of the thermocline. A possible evolution of the upper layers can be deduced from the Θ-S curves shown in Figure 10. Station 55 has not experienced any ice formation, and meltwater dominates. Station 58 is the actively convecting station, and the neighboring station 59 indicates lateral spreading of convected, cold water beneath a warmer layer and the beginning of the sharpening of the thermocline. Station 5 has experienced one winter convection, it has a temperature minimum located just above the thermocline, and the thermocline is slightly curved like an isopycnal. This indicates that the convection penetrates deeper into the thermocline than would be the case with mechanical mixing of meltwater into the Atlantic Water. The convection also creates that sharp bend in the Θ-S curve between the halocline and the thermocline, which is characteristic of the Arctic Ocean.

The mixed layer is created out of the upper, transformed part of the inflowing Atlantic Water. The depiction of Atlantic Water "diving" beneath outflowing low-salinity Polar Surface Water, as it enters the Arctic Ocean, is misleading. Shear may be present in the top few meters, though the thickness of the outflowing layer is not known. Thus while a thin upper part may move with the ice toward Fram Strait, most of the mixed layer must follow the inflowing Atlantic Water toward the east.

Ice melts during summer, followed by ice formation and homogenization during the next winter. North of the Barents and Kara Seas, winter convection reaches down to the thermocline,

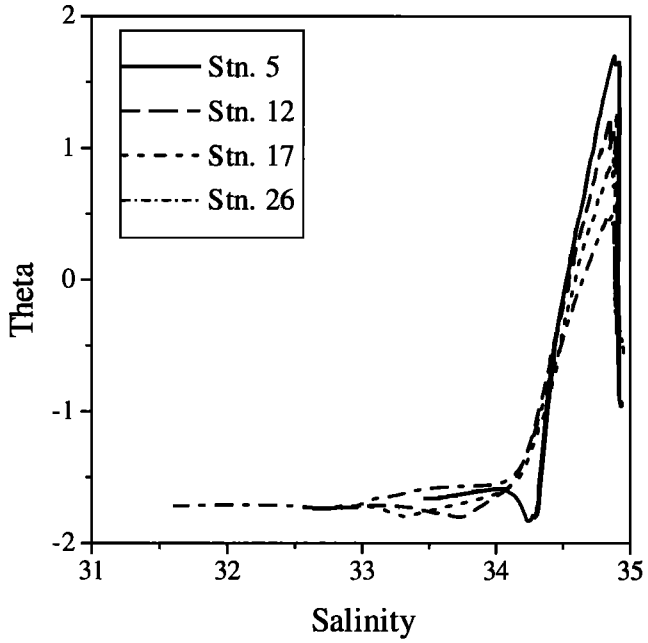

Figure 8. A Θ-S diagram showing *Oden* 91 stations 5, 12, 17, and 26 along section A. Note the temperature minimum on station 5.

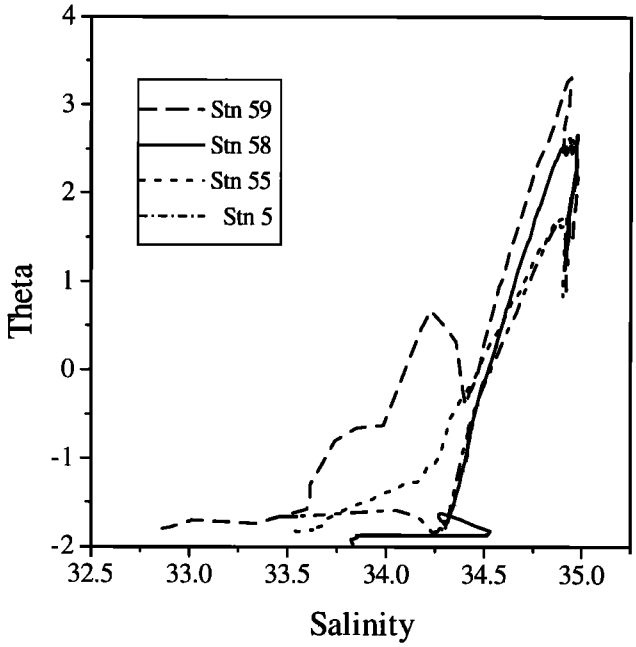

Figure 10. A Θ-S diagram from *Oden* 91 stations 55, 58, 59, and 5 suggesting a time evolution of the formation of the winter mixed layer north of Svalbard.

and heat from the Atlantic Layer may become entrained into the mixed layer. This heat eventually reaches the sea surface to be lost to ice melt or to the atmosphere. This agrees with the picture [*Treshnikov*, 1959] that the area between Svalbard and Severnaya Zemlya is a source region for the temperature minimum layer of the Eurasian Basin. After the mixed layer (S = 34.3) has formed above the thermocline, however, the entrainment from the Atlantic Layer appears to be small, since neither a large deepening nor a large increase in salinity is observed along the Eurasian slope (Figures 11a and 11b). Not until the boundary current reaches the eastern part of the Eurasian Basin does the mixed layer become capped by a larger fraction of low-salinity surface water originating from the river input [*Schauer et al.*, 1994]. The depth and salinity of the winter mixed layer is then drastically reduced (Figure 11c). The deepest part of the earlier mixed layer becomes isolated from the surface processes and turns into an intermediate "winter" halocline between the mixed layer and the thermocline.

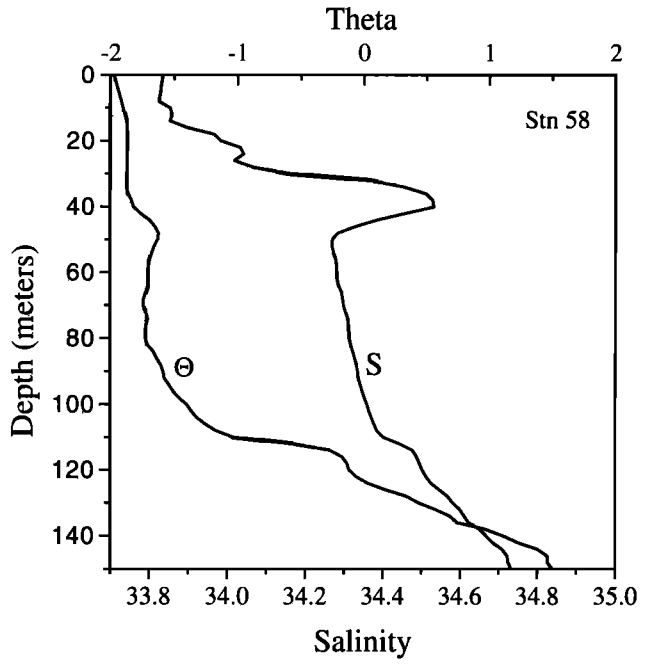

Figure 9. Temperature and salinity profiles for the upper 150 m of *Oden* 91 station 58 showing a strong positive salinity anomaly, indicating active convection.

The surface water moves in the Siberian Branch from the Laptev Sea toward Fram Strait, while the Atlantic Layer seems to split, with one part returning toward Fram Strait and the rest crossing the Lomonosov Ridge [*Rudels et al.*, 1994]. We expect the flow of the halocline to split like that of the Atlantic Layer. The halocline then acts as a trap for the heat lost upward by the Atlantic Layer, and its temperature slowly increases. The Θ-S curve moves away from the freezing line and attains the gentler bend observed in the Amundsen Basin (e.g., station 17 cf. station 5 in Figure 8).

Figure 12 shows the Θ-S curves from stations taken along two possible return paths of the surface water. Path 1 follows along the Amundsen Basin toward Fram Strait. Path 2 is traced by the water crossing the Lomonosov Ridge close to the North pole. A station (station 40) above the Morris Jesup Plateau has also been included. In these Θ-S diagrams the seasonal ice melt has been excluded for clarity, and the winter mixed layer is represented only by a single point.

Along the Amundsen Basin (path 1) the salinity of the mixed layer varies and the shape of the halocline changes. In the western part of the Amundsen Basin (stations 33 and 35) the mixed layer is fresher. This reflects the flow of Canadian Basin surface water, which crosses the Lomonosov Ridge to the west of section A, overriding the mixed layer of the Amundsen Basin. The salinity range of the halocline then increases, and the Amundsen Basin mixed layer can be observed as an upper temperature minimum within the halocline.

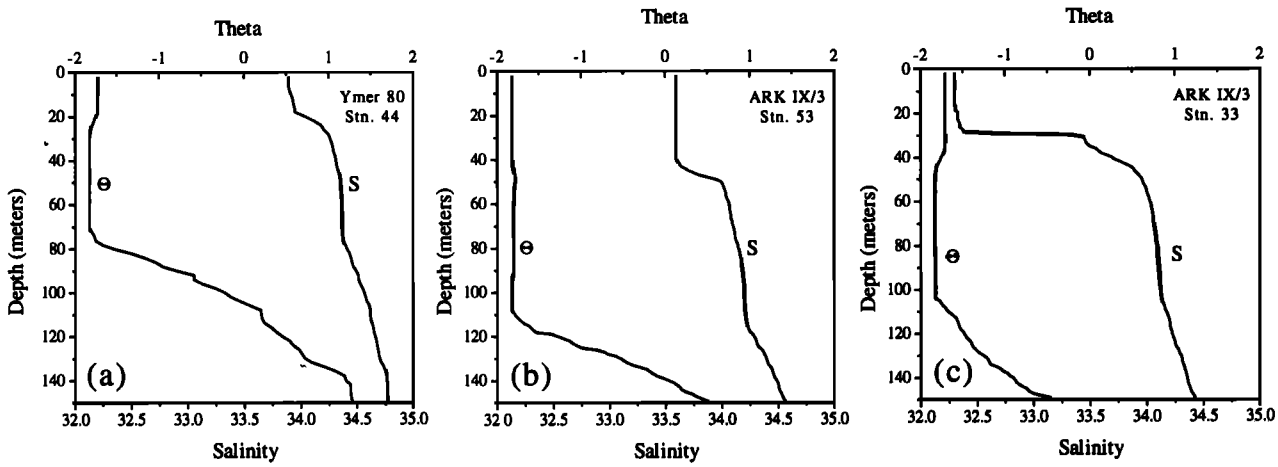

Figure 11. Temperature and salinity profiles for stations along the Eurasian continental slope: (a) *Ymer* 80 station 44 northwest of Frans Josef Land, (b) ARKTIS IX/4 station 53 northeast of Severnaya Zemlya, and (c) ARKTIS IX/4 station 33 north of the eastern Laptev Sea.

This pattern is supported by path 2, going from the Makarov Basin (station 27), over the North pole (station 29), down along the western Amundsen Basin (stations 38 and 45), toward Fram Strait. The halocline has a substantially larger salinity range, reflecting the fresh water added by river runoff and by the Bering Strait inflow to the Canadian Basin. The colder upper part of the halocline on stations 27, 38, and 45 suggests the presence of recently ventilated water. The winter mixed layer over the Lomonosov Ridge has a similar salinity (Table 1, stations 20-24) and could supply this upper part of the halocline. Station 29 has a much colder halocline, which is more akin to the one found on path 1. This indicates that the halocline waters cross the Lomonosov Ridge closer to Greenland than the surface water. Station 40 at the Morris Jesup Plateau contrasts sharply with station 29. The less saline surface water makes the salinity range of the halocline still larger, and its temperature is higher. This suggests a third stream crossing the Lomonosov Ridge closer to Greenland. The higher temperature is associated with a high silica content, indicating the presence of the nutrient maximum of upper halocline water from the Canada Basin [*Jones and Anderson*, 1986].

The horizontal distribution of the freshwater content and the thickness of the halocline are shown in Figure 13. The large increase in both thickness and freshwater content toward Greenland shows the result of the large influx of freshwater not only to the mixed layer, but also to the halocline in the Canadian Basin.

5. Discussion

The present approach has highlighted the importance of winter convection in the interior of the Arctic Ocean for forming the Arctic Ocean halocline. Shelf processes have not been discussed much. It is, however, commonly assumed and has also been

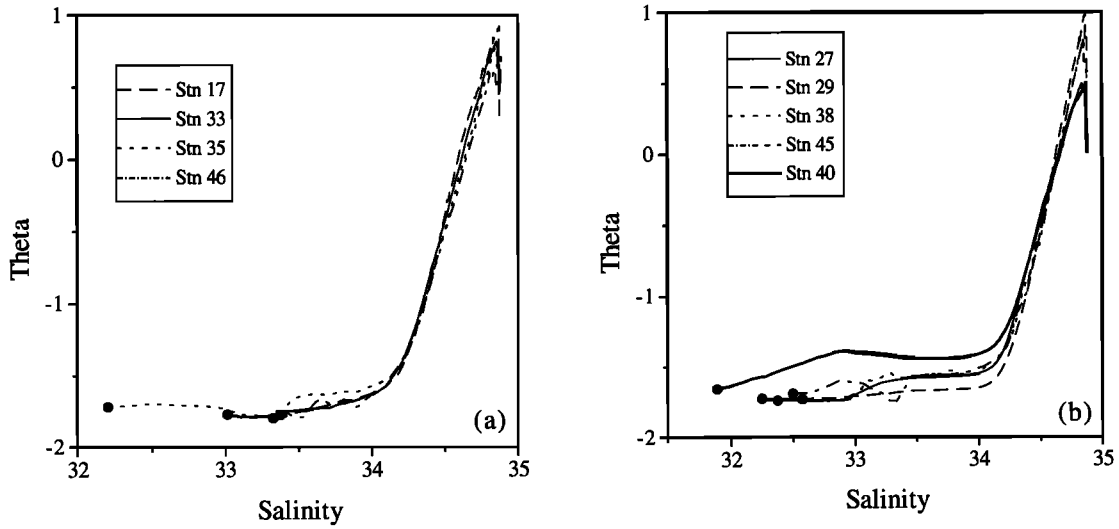

Figure 12. The Θ-S diagrams showing stations along different possible return paths of the flow of the upper layers toward Fram Strait (a) along the Amundsen Basin (*Oden* 91 stations 17, 33, 35, and 46) and (b) crossing the Lomonosov Ridge (*Oden* 91 stations 27, 29, 38, and 45.). The seasonal ice melt has been removed, and the stations only show the winter mixed layer as a dot. *Oden* 91 station 40, suggesting a third path, has been included in Figure 12b. For further information, see the text.

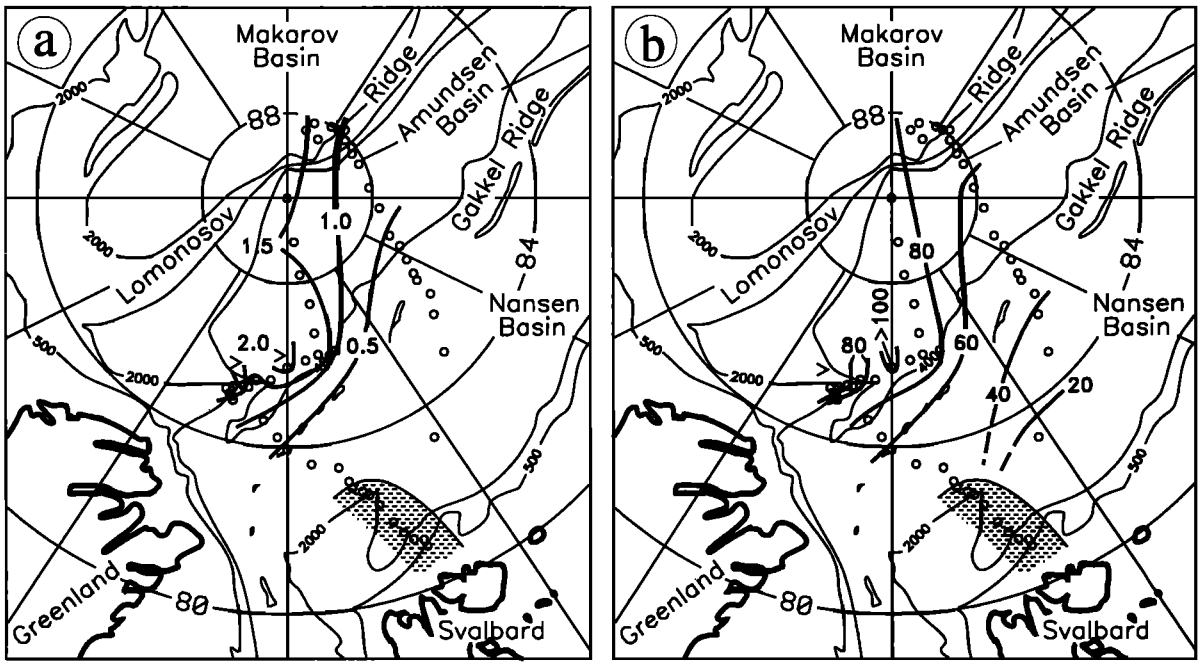

Figure 13. The horizontal distribution of (a) the freshwater content (meters) and (b) the thickness of the halocline (meters) in the western Eurasian Basin. The hatched areas indicate the presence of water which has not yet experienced a winter convection and where no winter mixed layer can be identified.

shown that dense water formed on the shelves does contribute to the halocline [*Aagaard et al.*, 1981; *Jones and Anderson*, 1986]. We shall therefore relate the present work to other models for the formation of the halocline. We shall also discuss the importance of the halocline for the exchanges between the deeper layers and the mixed layer in the Arctic Ocean.

5.1. Ice Formation on the Shelves

The possibility of creating dense water on the shelves comes about from their shallow water depth and from the formation of polynyas in the lee of islands and peninsulas [*Martin and Cavalieri*, 1989]. A larger fraction of open water favors strong ice formation and corresponding high brine production. Because of the shallow, solid bottom, high-salinity brine may accumulate during winter. However, as the bathymetry of the shelves varies, waters in a large density range will be produced. Shallow areas with high initial salinities can create water denser than what is found in the halocline [*Aagaard et al.*, 1985]. On the other hand, the shelf seas receive a large fraction of river runoff, and thus a large amount of ice has to form before a high salinity can be reached. In addition, the considerable width of the Arctic Ocean shelf areas implies a long passage to the shelf break. The dense shelf waters, initially formed and trapped on the shelves, will be diluted by mixing with water of lower salinity as they make their way to the deep basin.

The freshwater input to the Canadian Basin also reduces the salinity of the mixed layer. The salinity range of the halocline becomes larger, extending from $S \approx 34.3$ in the part supplied from the Eurasian Basin to $S < 32.5$ in the southern Canada Basin (Figure 2). This implies that several shelf sources may produce waters within that salinity range that then enter and augment the halocline. An example of shelf water penetrating into the halocline is the nutrient maximum associated with the "upper halocline" [*Jones and Anderson*, 1986]. Also, warmer, advective water such as the Bering Strait summer water will supply the halocline rather than the mixed layer, further increasing the thickness of the halocline.

The situation is different in the Eurasian Basin. The density range of the halocline is narrow, and the waters formed on the shelves by accumulation of saline brine are not likely to attain the halocline salinity exclusively. Waters that are slightly less dense will enter the mixed layer, while the high-salinity shelf water would sink deeper into the water column. The shelf process most frequently referred to; the creation of high-density water by brine rejection, is thus not likely to supply a large amount of water to the winter halocline in the Eurasian Basin. The strongest influence from the shelves on the halocline would be, instead, the influx of low-salinity water to the mixed layer north of the Laptev Sea. The second mechanism suggested for forming halocline water, forcing Atlantic Water onto the shelves where it loses heat to ice melt and to the atmosphere [*Coachman and Barnes*, 1962], could be important, however. A third mechanism that could contribute to the halocline arises because some of the inflow of Atlantic Water to the Arctic Ocean occurs via the Barents Sea. An encounter between Atlantic Water and sea ice, similar to the one north of Svalbard, takes place in the northern and eastern Barents Sea, and a deep mixed layer is created. The winter homogenization occurring in the northern Barents Sea would then result in similar or perhaps slightly higher salinities than those observed north of Svalbard [*Rudels et al.*, 1991].

The possibility that the densest part of the halocline is created by the melting of sea ice in the frontal zone between Atlantic Water and sea ice has been suggested by *Carmack* [1990] and has recently been elaborated by *Steele et al.* [1995]. *Steele et al.* [1995], following a work by *Moore and Wallace* [1988], relate the salinity change to the temperature reduction that would result from the melting of sea ice, and they obtain a mixing line that

then is taken to describe the formation and characteristics of the halocline water. The process is assumed to occur at the polar front, both in the Barents Sea and north of Svalbard. The observed mixing line between the mixed layer and the Atlantic Water is mostly more saline than the proposed line, but the water characteristics would deviate from the pure melting line if some oceanic sensible heat were lost to the atmosphere. *Steele et al.* [1995] assume that the partition of heat lost to ice melt and to the atmosphere varies over the year, with more heat going to melting ice in winter and to the atmosphere in summer. The observed salinity reflects the time-integrated result of the heat loss. They, however, do not consider, as is done here, the possibility of freezing to explain the curved shape of the thermocline and the location of the temperature minimum at salinities higher than those given by the proposed mixing line [*Steele et al.*, 1995, Plate 1].

5.2. Halocline Salinity

That oceanic sensible heat is lost both to ice melt and to the atmosphere when the mixed layer is formed could offer a clue to the salinity value $S \approx 34.3$ found at the base of the halocline north of the Barents, Kara, and Laptev Seas. In a work examining the heat exchange between the ocean, the ice cover, and the atmosphere during heat loss (B. Rudels, H. Friedrich, D. Hainbucher, and G. Lohmann, High latitude mixed layer in winter, manuscript in preparation, 1996), it was found that when ice is melting over warm water, the ice melt rate has a minimum if the fraction of the oceanic sensible het loss that goes into ice melt is equal to f_0:

$$f_o = \frac{2\alpha L}{\left[c(\beta S_2 - \alpha \Delta T)\right]} \tag{2}$$

Here α and β are coefficients of heat expansion and salt contraction, respectively. $L = 335\text{x}10^3$ J kg^{-1} is the latent heat of melting, and $c = 4190$ J °C^{-1} kg^{-1} is the heat capacity of seawater. S_2 is salinity of the Atlantic Water, and ΔT is the temperature differences between the Atlantic Water and the mixed layer. This relation is derived for the situation in winter. By assuming that the heat added to the ocean and the ice by radiation in summer only constitutes a perturbation (which is removed in fall) of the main ice melt caused by heat supplied from below, we could apply this expression to the formation of the winter mixed layer north of Svalbard. If the Atlantic Water has a temperature of 2.2°C and a salinity of 35 and the mixed layer is at freezing, ΔT becomes 4°C. The expansion coefficient of heat α is in this range $0.6\text{x}10^{-4}$, and β is $8\text{x}10^{-4}$, giving $f_0 = 0.35$. This value is close to the 40% going to ice melt found in the same region by *Steele et al.* [1995].

Since the only freshwater source for the mixed layer is the ice melt, the salinity S_1 of the mixed layer becomes (Rudels et al., manuscript in preparation, 1996)

$$S_1 = \frac{S_2}{\left(1 + \frac{f_o c \Delta T}{L}\right)} \tag{3}$$

which for the mixed layer at the freezing point gives $S_1 = 34.4$, close to the adopted value of 34.3. The mixed layer salinity depends upon the temperature of the Atlantic Water in the following two ways: through α, which decreases with decreasing temperature, and through ΔT. This means that a mixed layer formed by ice melt and homogenized by haline convection during freezing would have a higher salinity if the temperature of the underlying Atlantic Water were lower. This effect would dominate over a lower salinity of the Atlantic Water. The fact that the mixed layer found in the northern Barents Sea is more saline appears to support this conjecture [*Rudels et al.*, 1991, Figures 4, 5, and, 11; *Steele et al.*, 1995, Plate 1]. The processes occurring in the frontal zones between the Atlantic inflow and the sea ice then not only create the deep winter mixed layer forming the embryo of the halocline, but could also determine its initial Θ-S characteristics.

5.3. Vertical Exchanges

One of the more important effects of the halocline is that in the interior of the Arctic Ocean it acts as a trap for heat lost by the deeper layers, preventing heat from reaching the mixed layer and the sea ice. Mechanical stirring at the base of the mixed layer only entrains cold water into the mixed layer. The turbulent activity in the halocline is low, and the heat transfer from the Atlantic Layer to the halocline is primarily due to double-diffusive convection. Using our present observations, we estimate (1) the turbulent diffusion coefficient for salt (heat) at the base of the mixed layer and (2) the amount of heat that could be expected to be transferred from the Atlantic Layer into the halocline by double-diffusive convection.

The winter convection homogenizes the mixed layer down to the top of the halocline. We shall therefore look at the loss of salt from, or equivalently, the increase in fresh water in, the halocline. If the salinity loss is considered as a one-dimensional diffusion problem, the amount of salt that diffuses out of the halocline is [*Crank*, 1957]

$$M = 2\Delta S\sqrt{\left(\frac{Kt}{\pi}\right)} \tag{4}$$

where K is the turbulent diffusion coefficient, t is the time the diffusion has lasted, and ΔS is the salinity difference between the mixed layer and the top of the halocline when the diffusion starts. Since the salinity of the mixed layer is expected to change (because of the turbulent diffusion from below and, perhaps, also by a net annual formation of ice), this expression is not completely accurate. We use the salinity found at station 17 (Table 1) to determine ΔS. The amount of salt diffused out of the halocline is found from the amount of fresh water being added to the halocline and is given by

$$M = \text{fresh water x } 34.3 \tag{5}$$

Taking a salinity difference of 0.9 (from station 17 in Table 1) and a freshwater content in the halocline of 0.5 m and using the 8 years estimated by *Schlosser et al.* [1994] for the advection from the Laptev Sea to 30°E, we get $K = 1.1\text{x}10^{-6}$ m^2 s^{-1}. This is a small value, only 1 order of magnitude larger than the molecular diffusion coefficient. It is comparable to the $2\text{x}10^{-6}$ m^2 s^{-1} found by *Wallace et al.* [1987] but clearly smaller than the $5\text{x}10^{-5}$ m^2 s^{-1} proposed by *d'Asaro and Morison* [1992]. The diffusion coefficient could be even smaller, since ΔS may be underestimated. If the amount of salt, M, is added to a 60 m deep mixed layer, its salinity would increase by about 0.3. This would imply an initial ΔS of 1.2. The uncertainty of K is at least a factor of 2.

With K known it is possible to determine the penetration depth d of the diffusion into the halocline. Using the same time t, we find from

$$d = \sqrt{\pi K t} \quad (6)$$

d to be 30 m. This implies that the fresh water penetrates halfway to the base of the halocline.

The value obtained for the diffusion coefficient could tentatively also be used to assess the importance of the halocline for reducing the heat flux from the Atlantic Layer. If we remove the winter halocline, heat from the Atlantic Layer would be stirred directly into the mixed layer. Since the mixed layer is cooled to freezing in winter, the temperature at the top of the thermocline is constant and (4) holds. Taking the initial temperature difference to be $\Delta T = 4°C$, we find that 0.2×10^6 J m^{-2} has been added in 8 years. This implies an average heat transfer into the mixed layer of 1.26 W m^{-2}. This is close to the value 2 W m^{-2} often cited for the oceanic heat flux reaching the ice [*Maykut and Untersteiner*, 1971] and implies that the oceanic heat flux to the ice in the present-day Arctic Ocean is practically zero.

The heat lost upward by the Atlantic Layer would be trapped in the halocline. If this heat flux is due to double-diffusive convection, its magnitude can be estimated using the expression

$$Q = 0.058\left(\frac{\kappa_T^2 g\alpha}{\nu(1-\sqrt{\tau})}\right)^{\frac{1}{3}}\left[\Delta T(1-R_\rho\sqrt{\tau})\right]^{\frac{4}{3}} \quad (7)$$

[*Linden and Shirtcliffe*, 1978]. Here $\kappa_T = 10^{-7}$ and $\nu = 1.5 \times 10^{-6}$ m^2 s^{-1} are the molecular diffusion coefficients of heat and momentum, $\tau = \kappa_S \kappa_T^{-1} = 0.01$ is the ratio of the diffusion coefficients of salt and heat, and $R_\rho = \beta\Delta S(\alpha\Delta T)^{-1}$ is the stability ratio. Here ΔT is the temperature difference across a sharp gradient in the thermocline. If the total temperature and salinity differences between the Atlantic Layer and the halocline are 4°C and 0.7, respectively, the stability ratio becomes 2.35 using the same α and β as above. The temperature and salinity profiles shown in Figure 11c indicate that weak steps are present in the 100-m-thick thermocline. The average temperature step appears to be 0.1-0.2°C. Assuming an average value of 0.1 to take into account the reduction of the steps with time and inserting it into the expression above, we find that the double-diffusive heat flux becomes $Q_d = 1.3$ W m^{-2}. This is surprisingly high and close to the estimated heat flux into the mixed layer in the absence of a halocline. If the halocline is 50 m thick, this heat flux corresponds to a temperature increase of about 1.5°C. This implies a temperature of -0.4°C at the base of the halocline, which is 1°C higher than what is observed at station 17. This estimate, however, is very tentative, since not only does it involve assumptions about the temperature steps, but also it uses a theoretically derived expression for the double-diffusive fluxes that demands well mixed layers and sharp gradients. Such ideal conditions are not observed on the stations. In the present Arctic Ocean this heat would remain in the halocline. In the case of no halocline, as was considered above, temperature steps would be kept sharper, and larger double-diffusive fluxes were to be expected. This would substantially increase the estimate of oceanic heat flux to the mixed layer in the absence of a halocline.

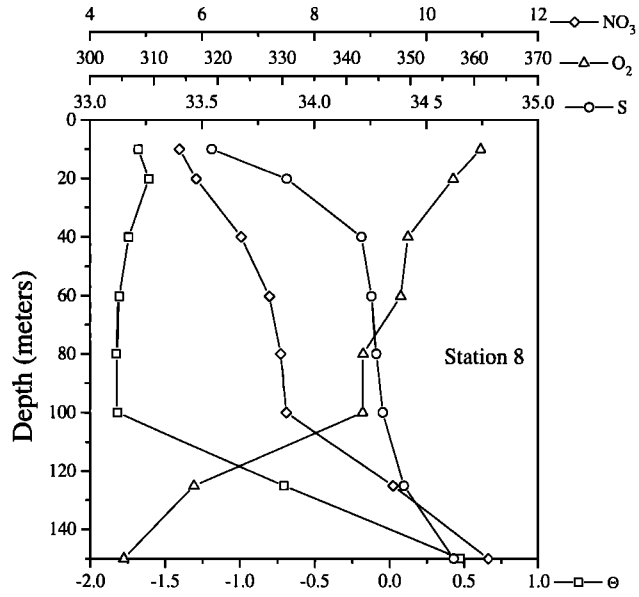

Figure 15. Profiles of temperature, salinity, oxygen and nitrate for *Oden* 91 station 8.

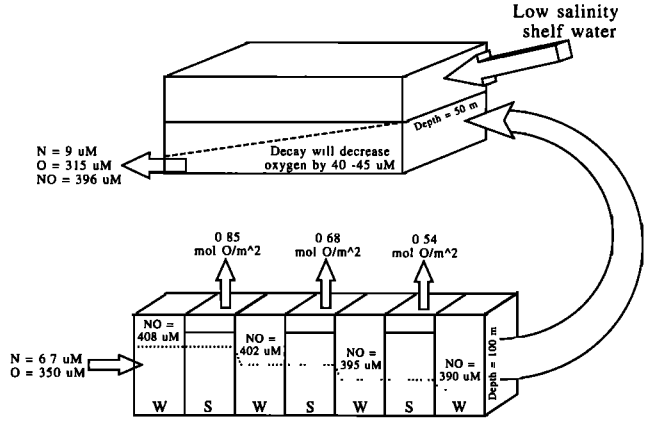

Figure 14. The effects of sea ice melt and winter convection on the oxygen and NO concentrations (micromoles per kilogram) of a parcel following the motion of the upper layer before and after it has been covered by the massive inflow of river runoff north of the Laptev Sea.

5.4. Formation of the Low NO Water

The seasonal evolution of the deep winter mixed layer on its route to the east, north of the Barents and Kara Seas, offers a possibility to form low NO water. In the eastern Eurasian Basin this water is covered by a low-salinity surface water originating in the Laptev Sea shelf (e.g., L.G. Anderson and K. Olsson, Input of dissolved carbon to and biogeochemical transformation of carbon in the Arctic shelf seas, submitted to Continental Shelf Research, 1995). The low-salinity shelf water presumably has a high annual mean nutrient content but not much oxygen depletion. Hence when this water flows on top of the low NO water, an apparent NO minimum is formed.

A schematic illustration of the low NO formation is presented in Figure 14. The initial nitrate and oxygen concentrations of the winter mixed layer (S = 34.3) formed north of Svalbard are taken to be the average concentrations of the upper 100 m of station 8 (Figure 15), i.e., 6.7 and 350 μmol kg^{-1}, respectively. After the first winter it is assumed that primary production in a 20 m thick surface layer consumes all available nitrate. The oxygen concentration is kept at 100% saturation (268 μmol kg^{-1} at S=34.3 and freezing temperature), resulting in an out gassing to the atmosphere. The possibility that this exact scenario is

attained is unlikely, but it is not critical for the discussion. During the next winter the upper 100 m is again homogenized, giving lower NO values compared with the previous winter. The process is repeated each year until the water parcel arrives at the eastern Eurasian Basin. This process may occur both in the Nansen Basin and north of the polar front in the Barents Sea, with a production of low NO water in the Barents Sea not being precluded. Once the winter mixed layer reaches the eastern Eurasian Basin, it is covered by a low-salinity surface layer (of shelf origin), shielding the low NO water from the atmosphere and making NO a conservative parameter.

With this picture in mind we examine the stages of the evolution of the NO minimum in the halocline. The changes in the oxygen, nitrate, and NO concentrations in the winter mixed layer are summarized in Table 2. With the assumptions made above and with plausible values of primary productivity, 3 years is long enough to attain the NO concentration found in the NO_{min} water of the *I/B Oden* 1991 cruise stations 15 - 20 in the Amundsen Basin. Table 2 also includes the amount of oxygen escaping to the atmosphere from the summer mixed layer, as well as the amount of nitrogen fixed in organic matter and the corresponding primary productivity, expressed in g C m^{-2}. The primary productivity values are high for an ice-covered region, but as stated above, it is unlikely that all nitrogen is consumed in the summer mixed layer. In order to reach the NO_{min} concentration observed in the western Amundsen Basin using a lower primary productivity, the winter mixed layer would have to experience more seasons on its route to the eastern Eurasian Basin. A mean current of 1 to 2 cm s^{-1} would give a transit time of 3 to 5 years.

North of the Laptev Sea, the low NO water constitutes a layer about 50 m thick (station 33, Figure 11c). Low-salinity surface water with a different NO concentration is mixed into the top of this layer during its transit to the west, thus causing the NO_{min} to be restricted to the bottom of the winter halocline. The chemical signature of the winter halocline is affected by decay of organic matter added to the water column, either by advection from the shelves or by particles sinking down from the ice and/or surface layer. The amount of organic matter needed to produce the concentrations of the western Amundsen Basin, assuming a constant decay rate over the initial 50-m layer, is 20 to 22 g C m^{-2}. These numbers have to be divided by the transit time along the basin to get annual estimates. Calculations using the helium 3 signature give 8-15 years for the transit time of waters in the salinity range 34.0 to 34.4 [*Schlosser et al.*, 1994], resulting in an annual supply of 1 - 3 g C m^{-2}.

The above mechanism can also explain the existence of several other observed low NO water masses having lower salinity.

Table 2. Evolution With Time of Some Chemical Constituents in the Winter Mixed Layer of the Model

Year	O_2	NO_3	NO	O_2 Loss	N Assimilation	Primary Productivity
1	350.0	6.7	408.0	0.85	0.13	11.36
2	353.6	5.4	401.8	0.68	0.11	9.09
3	356.5	4.3	395.1	0.54	0.09	7.27
4	358.8	3.4	389.7	0.43	0.07	5.82
5	360.6	2.7	385.3	0.35	0.05	4.65

See Figure 14 (bottom). Units for O_2, NO_3 and NO are micromoles per kilogram; for O_2-loss and N-assimilation, moles per square meter; and for primary productivity, g C m^{-2}.

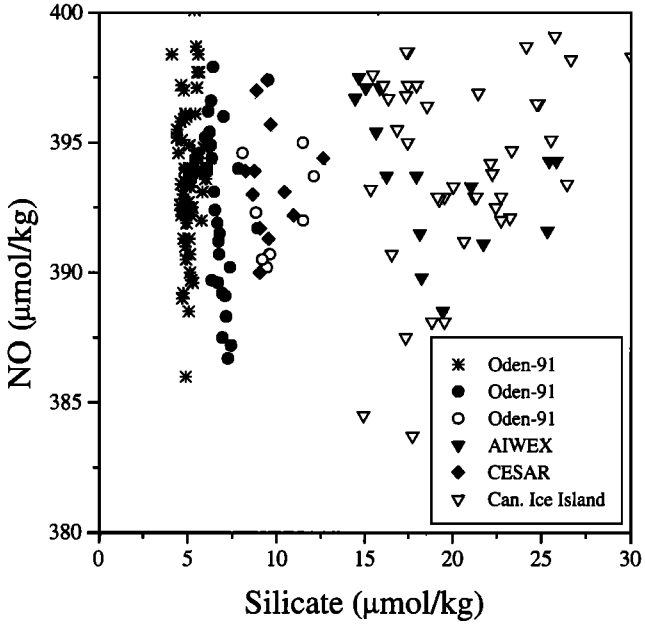

Figure 16. NO versus silicate for samples with 34 < S < 34.5 and NO < 400. *Oden* 91 stations 8-23, 29-35, and 47-50 are stars; *Oden* 91 stations 24-28, 36-39, and 45-46 solid circles; *Oden* 91 Stations 40-44, open circles; AIWEX stations, solid triangles; CESAR stations, solid diamonds; and the Canadian Ice Island, open triangles.

Examples of these are the surface water at the *I/B Oden* 1991 cruise stations 13, 17, 20, and 28, as well as upper waters in Siberian shelf seas [*Wilson and Wallace*, 1990].

A minimum in NO at a salinity of about 34.3 observed in the Canadian Basin has been used as a tracer of halocline water originating in the Eurasian Basin [e.g., *Jones and Anderson*, 1986; *Salmon and McRoy*, 1994]. While the NO_{min} does seem to pinpoint the source region of this halocline water, by itself it cannot be used to trace the halocline circulation. *Rudels et al.* [1994] used the silicate concentrations in the Atlantic Layer and intermediate depth waters to propose a circulation scheme for these waters. We follow a similar procedure for the NO_{min}.

High-salinity shelf water, having high silicate concentration, enters the Canadian Basin in the region north of the Chukchi Sea [*Jones and Anderson*, 1986]. *Rudels et al.* [1994] argued that this near-surface silicate is transported into deeper regions by slope plumes triggered by the high density of the shelf water. These plumes can penetrate to all depths of the Canadian Basin, resulting in elevated silicate concentrations.

The Eurasian Basin halocline, with NO values less than 400 µmol kg^{-1}, has salinities between 34.0 and 34.5. When all silicate observations from the *I/B Oden* 1991 cruise satisfying these criteria are plotted, they fall into three classes (Figure 16). The data from stations 8-23, 29-35, and 47-50 have the lowest silicate concentration, the data from stations 24-28, 36-39, and 45-46 have intermediate concentrations, while those from stations 40-44 have the highest concentrations. Included in Figure 16 are also data in the same salinity interval from the ice stations Canadian Expedition to Study the Alpha Ridge (CESAR), AIWEX, and Canadian Ice Island (see Figure 1 for positions). This distribution suggests that the circulation pattern for the low NO halocline is similar to the underlying Atlantic Layer [*Rudels et al.*, 1994]. The low NO halocline forms in the Eurasian Basin and passes to the east north of the Kara and Laptev Seas, with

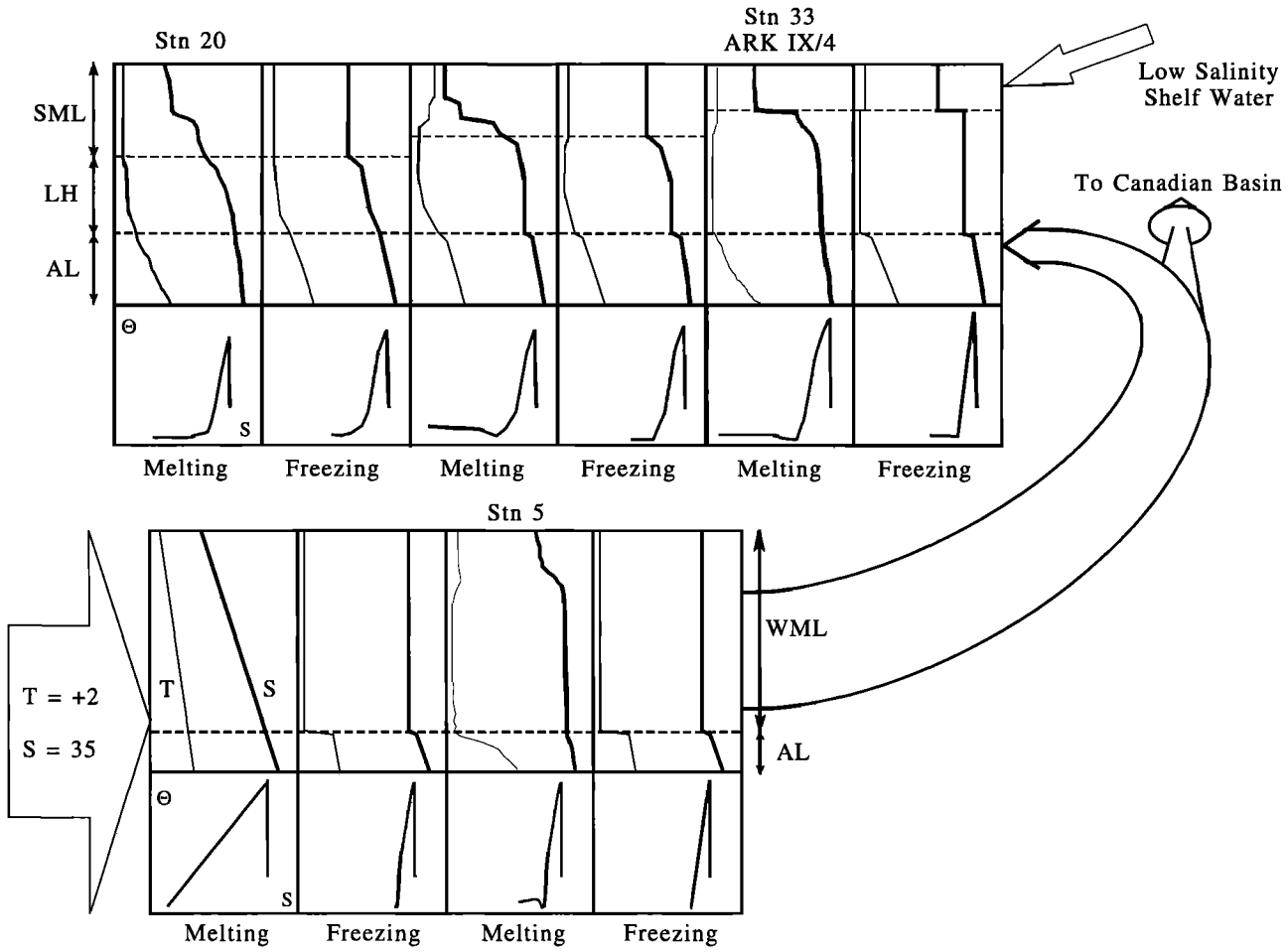

Figure 17. The evolution of the Arctic Ocean surface water and halocline. Schematic profiles and Θ-S diagrams with presumed and measured properties (stations 5, 33, and 20) illustrating the evolution of the upper layers of the Eurasian Basin as a result of the combined effects of winter convection and summer icemelt, input of river runoff, and the general circulation.

one part turning at the Lomonosov Ridge and one part continuing into the Canadian Basin. There are two outflows from the Canadian Basin identifiable near the Morris Jesup Plateau. The highest silicate concentrations, found at AIWEX and the Canadian Ice Island, are, however, not seen in the *I/B Oden* 1991 cruise data. The high-silicate water found at the AIWEX site suggests the existence of a second gyre in the Canada Basin whose water will exit along the continental slope, closer to Greenland, than the region sampled during the *I/B Oden* 1991 cruise. The Atlantic Layer under the NO halocline at AIWEX also has higher silicate values than were observed in the Atlantic Layer at our stations near the Morris Jesup Plateau. Given the similarities between the silicate distribution in the low NO halocline and the Atlantic Layer, one might speculate that a second gyre exists in the Atlantic Layer in the Canada Basin in addition to that depicted by Rudels et al. [1994].

6. Summary

The present work has shown that the formation of the Arctic Ocean halocline involves a number of processes that closely relate the circulation to the input of fresh water from river runoff and to the freezing and melting of sea ice. These different processes and our perception of the evolution of Arctic Ocean surface waters and halocline are represented in Figure 17. Initially, north of Fram Strait, sea ice melts as it encounters inflowing Atlantic Water. A low-salinity surface layer is created that is homogenized in winter by haline convection into a deep mixed layer. This mixed layer flows eastward above the core of the Atlantic Layer. During subsequent summers, ice melts, the meltwater again is removed by freezing in winter, and the deep mixed layer extending down into the thermocline is maintained. When the boundary current reaches the eastern Eurasian Basin, it receives an injection of low-salinity shelf water caused by the large river input from Ob, Yenisey, and Lena accumulating in the Laptev Sea. The mixed layer becomes less saline and the winter convection shallower. A winter halocline is formed between the mixed layer and the thermocline. The boundary current splits north of the Laptev Sea, with one part returning toward Fram Strait and the other crossing the Lomonosov Ridge into the Canadian Basin.

Brine rejection on the shelves produces waters of varying salinities, which will be distributed over the entire water column. Because of the narrow density range of the halocline north of the shelves of the Eurasian Basin, the contribution to the halocline from these shelves will be small. This is not the case in the Canadian Basin. There the halocline initially has a substantial density range (about as large as that of the deeper part of the water column) as it enters across the Lomonosov Ridge, north of the Laptev Sea. Within the Canadian Basin its upper boundary gradually becomes less saline because of further influx of river water.

On the return path along the Amundsen Basin the seasonal melting and freezing continue. The salinity of the mixed layer likely increases somewhat because of turbulent diffusion from below and, perhaps, because of net ice formation. The thickness of the mixed layer and the halocline remain constant until the return flow converges with waters returning from the Canadian Basin.

A significant outflow of the upper layers of the Canadian Basin takes place through the Canadian Arctic Archipelago, but a part crosses the Lomonosov Ridge into the western Eurasian Basin, mainly as a boundary current along the American continental slope. Some of the surface water, however, appears to follow the sea ice of the transpolar drift and passes over the North pole toward Fram Strait. This water overrides the mixed layer of the Amundsen Basin and shows up as an increase in halocline thickness and salinity range. The low-salinity surface layer protects the halocline in the boundary current. If part of the upper halocline water from the Canadian Basin were deflected out of the boundary current, it would become exposed to the winter convection and incorporated into the mixed layer. The boundary between the return flows from the Canadian Basin and along the Amundsen Basin is thus a region where a mechanism capable of eroding parts of the halocline may operate in contrast to the continuous buildup occurring elsewhere in the Arctic Ocean.

The halocline acts as a trap for the upward transfer of heat from the Atlantic Layer and its temperature increases from below. Because of turbulent mixing between the mixed layer and the halocline, fresh water is stirred into the halocline from above. Observed changes in temperature and salinity have been used to estimate both a turbulent diffusion coefficient K and the heat transfer due to double-diffusive convection. The value 1.1×10^{-6} m^2 s^{-1} for the turbulent diffusion coefficient K is small. The observed increase in temperature at the base of the halocline is less than what is predicted by the applied, double-diffusive flux law.

Acknowledgments. This work was done with financial support from the Deutsche Forschungsgemeinschaft, SFB 318 (B.R.), the Swedish Natural Science Research Council (L.G.A.), and the Panel on Energy Research and Development, Canada (E.P.J.).

References

Aagaard, K., L.K. Coachman, and E. Carmack, On the halocline of the Arctic Ocean, *Deep Sea Res.,Part A, 28*, 529-545, 1981.

Aagaard, K., J.H. Swift, and E.C. Carmack, Thermohaline circulation in the Arctic Mediterranean Seas, *J. Geophys. Res., 90*, 4833-4846, 1985.

Anderson, G.C., and J.H. Swift, Arctic Internal Waves Experiment (AIWEX) hydrographic data, March 24-April 25, 1985, *Publ. Ref. 90-10*, Scripps Inst. of Oceanogr., Univ. of Calif., San Diego, La Jolla, 1990.

Anderson L.G., G. Björk, O. Holby, E.P. Jones, G. Kattner, K.P. Koltermann, B. Liljeblad, R. Lindegren, B. Rudels, and J. Swift, Water masses and circulation in the Eurasian Basin: Results from the *Oden* 91 expedition, *J. Geophys. Res., 99*, 3273-3283, 1994.

Bauch, D, P. Schlosser, and R.G. Fairbanks, Freshwater balance and the sources of deep and bottom waters in the Arctic Ocean inferred from the distribution of $H_2{}^{18}O$, *Prog. in Oceanogr., 35*, 53-80, 1995.

Broecker, W.S., "NO," A conservative-mass tracer, *Earth Planet. Sci. Lett., 23*, 100-107, 1974.

Carmack, E.C., Large-scale physical oceanography of Polar oceans, in *Polar Oceanography, Part A*, edited by W.O. Smith Jr., pp. 171-212, Academic, San Diego, Calif., 1990.

Coachman, L.K., and C.A. Barnes, Surface water in the Eurasian Basin of the Arctic Ocean, *Arctic, 15*, 251-277, 1962.

Crank, Mathematics of Diffusion, Oxford Univ. Press, New York, 1957.

d'Asaro, E.A., and J.H. Morison, Internal waves and mixing in the Arctic Ocean, *Deep Sea Res. Part A, 39*, S459-S484, 1992.

Defant, A., *Physical Oceanography*, vol. 1. 729 pp., Pergamon, Tarrytown, N.Y., 1961.

Jones, E.P., and L.G. Anderson, On the origin of the chemical properties of the Arctic Ocean halocline, *J. Geophys. Res., 91*, 10,759-10,767, 1986.

Linden, P.F., and T.G.L. Shirtcliffe, The diffusive interface in double-diffusive convection, *J. Fluid Mech., 87*, 417-432, 1978.

Martin, S., and D.J. Cavalieri, Contributions of the Siberian shelf polynyas to the Arctic Ocean intermediate and deep water, *J. Geophys. Res., 94*, 12,725-12,738, 1989.

Maykut, G.A., and N. Untersteiner, Some results from a time dependent, thermodynamic model of sea ice, *J. Geophys. Res., 76*, 1550-1575, 1971.

McPhee, M.G., The upper ocean, in *The Geophysics of Sea Ice*, edited by N. Untersteiner, pp. 339-394, Plenum, New York, 1986.

Melling, H., and E.L. Lewis, Shelf drainage flows in the Beaufort Sea and their effects on the Arctic Ocean pycnocline. *Deep Sea Res., Part A, 29*, 967-985, 1982.

Moore, R.M., and D.W.G. Wallace, A relationship between heat transfer to sea ice and temperature-salinity properties of the Arctic Ocean waters, *J. Geophys. Res, 93*, 565-571, 1988.

Östlund, H.G., and G. Hut, Arctic Ocean water mass balance from isotope data, *J. Geophys. Res., 89*, 6373-6381, 1984.

Rudels, B., A.-M. Larsson, and P.-I. Sehlstedt, Stratification and water mass formation in the Arctic Ocean: Some implications for the nutrient distribution, *Polar Res., 10*, 19-31, 1991.

Rudels, B., E. P. Jones, L. G. Anderson, and G. Kattner, On the origin and circulation of Atlantic layer and intermediate depth waters in the Arctic Ocean, in *The Polar Oceans and Their Role in Shaping the Global Environment, Geophys. Monogr. Ser.*, vol. 85, edited by O. M. Johannessen, R. D. Muench, and J. E. Overland, pp. 33-46, AGU, Washington, D.C., 1994.

Salmon, D.K., and C.P. McRoy, Nutrient-based tracers in the western Arctic: A new Lower Halocline Water defined, in *The Polar Oceans and Their Role in Shaping the Global Environment, Geophys. Monogr. Ser.*, vol. 85, edited by O. M. Johannessen, R. D. Muench, and J. E. Overland, pp. 47-62, AGU, Washington, D.C., 1994.

Schauer, U., B. Rudels, R.D. Muench, L. Timokhov, H. Witte, and G. Lohmann, First results of the CTD measurements, in *Die Expedition ARCTIC 93 Der Fahrtabschnitt ARK-IX/4 mit FS "Polarstern" 1993*, edited by D. Fütterer, pp. 27-31, *Ber. Polarforschung, 149*, Alfred Wegner Inst., Bremerhaven, Germany, 1994.

Schlosser, P., D. Bauch, R. Fairbanks, and G. Bönisch, Arctic river-runoff: Mean residence time on the shelves and in the halocline, *Deep- Sea Res., Part I, 41*, 1053-1068, 1994.

Steele, M., J.M. Morison, and T.B. Curtin, Halocline water formation in the Barents Sea, *J. Geophys. Res., 100*, 881-894, 1995.

Treshnikov, A.F., Poverkhnostniye vodi v arkticheskom basseinie, *Probl. Arkt. Antarkt., 7*, 5-14, 1959.

Treshnikov, A.F., and G.I. Baranov, Structure of water circulation and dynamics of the water budget of the north polar region, *Probl. Arkt. Antarkt., 47*, 93-100, 1976.

Untersteiner, N., On the ice and heat balance in Fram Strait, *J. Geophys. Res., 93*, 527-531, 1988.

Vowinckel, E., and S. Orvig, The climate of the North Polar Basin, in *World Climate Survey*, vol. 14, *Climates of the Polar Regions* edited by S. Orvig, pp. 129-252, Elsevier, New Yourk, 1970.

Wallace, D.W.R., R.M. Moore, and E.P. Jones, Ventilation of the Arctic Ocean cold halocline: Rates of diapycnal and isopycnal transport, oxygen utilization, and primary production inferred using chlorofluoromethane distributions, *Deep Sea Res., Part A, 34*, 1957-1979, 1987.

Wilson, C., and D.W.R. Wallace, Using the nutrient ratio NO/PO as a tracer of continental shelf waters in the central Arctic Ocean, *J. Geophys. Res., 95*, 22,193-22,208, 1990.

L.G. Anderson, Department of Analytical and Marine Chemistry, Göteborg University, S-412 96 Göteborg, Sweden. (e-mail: leif@amc.chalmers.se)

E.P. Jones, Department of Fisheries and Oceans, Bedford Institute of Oceanography, P. O. Box 1006, Dartmouth, N.S., Canada B2Y 4A2. (email: p_jones@bionet.bio.dfo.ca)

B. Rudels, Institut für Meereskunde, Universität Hamburg, Troplowitzstraße 7, D-22529 Hamburg, Germany. (email: rudels@ifm.uni-hamburg.de)

(Received July 25, 1995; revised January 2, 1996;
accepted January 2, 1996.)